SARS-CoV-2 Intra-host Evolution Is Not Favoured by Immune System Deficiencies

Laura Manuto , Martina Bado , Marco Cola , Elena Vanzo , Maria Antonello , Giorgia Mazzotti , Monia Pacenti , Giampaolo Cordioli , Lolita Sasset , Anna Maria Cattelan , Stefano Toppo * , Enrico Lavezzo *

Posted Date: 4 December 2023

doi: 10.20944/preprints202312.0174.v1

Keywords: SARS-CoV-2 genomic variability; viral quasispecies; immunocompromised subjects; intra-host

Article

SARS-CoV-2 Intra-Host Evolution Is Not Favoured by Immune System Deficiencies

Laura Manuto [1,†], Martina Bado [1,†], Marco Cola [1], Elena Vanzo [1], Maria Antonello [1], Giorgia Mazzotti [1], Monia Pacenti [2], Giampaolo Cordioli, Lolita Sasset [2], Anna Maria Cattelan [1,2], Stefano Toppo [1,*,‡] and Enrico Lavezzo [1,*,‡]

[1] University of Padova, Padova, Italy; laura.manuto@phd.unipd.it (L.M.); martina.bado@studenti.unipd.it (M.B.); elena.vanzo.1@studenti.unipd.it (E.V.); maria.antonello@studenti.unipd.it (M.A.); giorgia.mazzotti@studenti.unipd.it (G.M.); marco.cola@studenti.unipd.it (M.C.); giampaolo.cordioli@studenti.unipd.it (G.C.), lolita.sasset@aopd.veneto.it (L.S.), stefano.toppo@unipd.it (S.T.), enrico.lavezzo@unipd.it (E.L.)

[2] University Hospital of Padova, Padova, Italy; monia.pacenti@aopd.veneto.it (M.P.); annamaria.cattelan@aopd.veneto.it (A.M.C.)

* Correspondence: enrico.lavezzo@unipd.it (E.L.); stefano.toppo@unipd.it (S.T.)

† These authors contributed equally to this work.

‡ Authors jointly supervised this work.

Abstract: During the COVID-19 pandemic, immunosuppressed patients showed prolonged SARS-CoV-2 infections, with several studies reporting the accumulation of mutations in the viral genome. The weakened immune system present in these individuals, along with the effect of antiviral therapies, are thought to create a favourable environment for intra-host viral evolution and have been linked to the emergence of new viral variants, which strongly challenged the containment measures and some therapeutic treatments. To assess whether an impaired immunity could lead to an increased instability of viral genomes, longitudinal nasopharyngeal swabs were collected from eight immunocompromised patients and fourteen non-immunocompromised subjects, all undergoing SARS-CoV-2 infection. Intra-host viral evolution was compared between the two groups through deep sequencing, exploiting a probe-based enrichment method to minimize the possibility of artefactual mutations commonly generated in amplicon-based methods, which heavily rely on PCR amplification. Although, as expected, immunocompromised patients experienced significantly longer infections, the acquisition of novel intra-host viral mutations was similar between the two groups. Moreover, a thorough analysis of viral quasispecies showed that the variability of viral populations in the two groups is comparable not only at the consensus level, but also when considering low frequency mutations. This study suggests that a compromised immune system alone does not affect SARS-CoV-2 within-host genomic variability.

Keywords: SARS-CoV-2 genomic variability; viral quasispecies; immunocompromised subjects; intra-host

1. Introduction

Since the beginning of the SARS-CoV-2 pandemic, several studies emphasized a prolonged positivity of RT-PCR tests in the immunosuppressed population, which can be explained by impairment of viral clearance by weakened innate and adaptive immune responses in immunocompromised patients [1]. Although a positive RT-PCR test only reflects the detection of viral RNA and does not necessarily indicate the presence of active viral replication or infectivity [2], the specific host environment of immunocompromised subjects has been suggested to be responsible of an accelerated viral evolution [1,3] or to induce the selective accumulation of viral mutations in genomic regions that affect viral fitness, promoting immune system escape and transmission [4–7]. In addition to the compromised immune system, also typical treatments, such as convalescent

 doi:10.20944/preprints202312.0174.v1

plasma, monoclonal antibodies or antivirals, have been reported to induce selective pressure on SARS-CoV-2 intra-host evolution [5,8–11]. Moreover, protracted SARS-CoV-2 infections in immunocompromised subjects have been indicated as the possible source for the origin of novel SARS-CoV-2 variants, namely B.1.1.7 (Alpha) [7] and of B.1.1.529 (Omicron) [6], due to the high difference in the number and location of mutations compared with the viral haplotypes circulating at the time, according to sequence availability in public databases. However, most of the available data is based on case studies of immunocompromised subjects who were monitored due to recurrent or prolonged hospitalisation, whereas very few longitudinal studies have been performed on immunocompetent subjects [12–16]. Nonetheless, those studies reported the longitudinal accumulation of novel SARS-CoV-2 mutations affecting viral fitness and immune escape in non-immunocompromised subjects as well. Very few studies currently available have assessed intra-host SARS-CoV-2 evolution in immunocompromised and non-immunocompromised subjects [15,16].

In this study, we used a whole genome deep sequencing approach on serial nasopharyngeal swab samples collected from immunosuppressed and non-immunocompromised patients, treated with antiviral agents or monoclonal antibodies, with the aim of investigating SARS-CoV-2 intra-host evolution and assessing the potential role of a compromised immune system in driving the accumulation of mutations, both quantitatively and qualitatively. Samples collected the day of the first positive SARS-CoV-2 test (T0), and after 3 (T3), 7 (T7), 14 (T14), 21 (T21) and 30 (T30) days, according to infection length, were deep sequenced and analysed for longitudinal viral haplotype variation and for low frequency mutations diversity and shifts. Given that there are no standard guidelines to study low frequency variants, we decided to rely on a capture-based protocol that was recently proven to be sensitive and efficient in providing an unbiased full coverage and a reliable representation of low frequency variants [17–19]. Moreover, we minimised the number of PCR cycles normally required by the protocol to avoid the generation of artefacts commonly associated with amplicon sequencing. In addition, a subset of samples was sequenced twice to allow a precise calibration of the parameters to reliably call the low frequency variants.

2. Materials and Methods

2.1. Patients and samples

We conducted a single-centre prospective study at Padova University Hospital from December 2021 to April 2022. A group of eight immunocompromised and a group of fourteen non-immunocompromised adult subjects, positive to SARS-CoV-2, were enrolled among those evaluated at the outpatient clinic for COVID-19 early treatment. All participants underwent regular nasopharyngeal swabs for the detection of SARS-CoV-2 at 3, 7, 14, 21 and 30 days after the first positive test, or until negativization. The enrolled patients were prescribed antiviral therapy (remdesivir, or monoclonal antibodies) in accordance with the criteria outlined in the Italian guidelines. Individuals were divided in two groups: severe immunocompromised patients (Group 1) and non-immunocompromised patients but at high risk of COVID-19 clinical progression (Group 2) [20].

SARS-CoV-2 genome was searched with Simplexa™ COVID-19 Direct assay (DiaSorin) targeting S gene and ORF1ab gene, following manufacturer instructions. After inactivating nasopharyngeal swab samples at 90 °C for 30min, total nucleic acids were purified using a MagNA Pure 96 System (Roche Applied Sciences) following manufacturer instructions.

The study was performed according to the ethical guidelines of the Declaration of Helsinki (7th revision). All the patients gave their written informed consent and all analyses were carried out on anonymized data as required by the Italian Data Protection Code (Legislative Decree 196/2003) and the general authorization issued by the Data Protection Authority.

2.2. Library Construction, and Sequencing Methods

The sequencing libraries were prepared in accordance with the protocol "Creating cDNA libraries using Twist library preparation kit for ssRNA virus detection for use with target enrichment workflow" and enriched with Twist SARS-CoV-2 Research Panel. Samples were treated with DNAse

 doi:10.20944/preprints202312.0174.v1

in order to eliminate DNA, and quantified with Qubit RNA High Sensitivity assay. RNA samples were then diluted and cDNA was synthetized and quantified with Qubit DNA High Sensitivity assay. Samples were enzymatically fragmented, end-repaired and dA-tailed in order to generate dA-tailed DNA fragments with average size of 300bp. Ligation of TWIST Universal Adapters and purification was performed. Adapted cDNA libraries were amplified with Twist Unique Dual Index Primers (10 PCR cycles), purified and quantified with Qubit DNA High Sensitivity assay. The resulting libraries were validated using the Fragment Analyzer (High Sensitivity Small Fragment Analysis Kit) to check size distribution. An equal amount of the indexed libraries was pooled to reach a total mass of 1500ng. Each pool was hybridized with SARS-CoV-2 probes and the capture was amplified (9 PCR cycles) and purified with Ampure beads. The resulting libraries were validated using the Fragment Analyzer (High Sensitivity Small Fragment Analysis Kit) to check size distribution. The concentration of the libraries was defined on the basis of the Qubit 4.0 Fluorometer. The libraries were normalized to 4 nM and loaded at a concentration of 1,2 pM onto an Illumina Mid Output Flowcell with 1% of Phix control. The samples were then sequenced with NextSeq, using the Illumina V2 chemistry, 2 × 150 bp paired end run.

2.3. Viral Genome Assembly: Quality Check and Mapping of the Reads

The raw sequences were filtered for length and quality with Trimmomatic [21] v0.39 according to the following parameters: ILLUMINACLIP:TruSeq3-PE-2:2:30:10, LEADING:30, TRAILING:30, SLIDINGWINDOW:4:20, and MINLEN:40. High quality reads were aligned on the SARS-CoV-2 reference genome (genbank ACC: NC_045512) with BWA-MEM v0.7.17. Duplicated reads were then removed with Picard tool v3.0.0 (http://broadinstitute.github.io/picard/, accessed on 10 May 2023). Consensus sequences were generated using a combination of SAMtools [22] v1.11 and VarScan [23] v2.4.4 variant caller (http://varscan.sourceforge.net). First all bam files were cleaned from secondary alignments, incorrectly mapped reads, low quality reads and unpaired reads. The consensus sequences were then reconstructed by utilising VarScan with no filters to call all the identified bases and variants per each genomic position. Subsequently, the output was filtered by an in-house Python script that required a minimum of 5 reads to call a base, at least 2 forward and 2 reverse reads and a frequency greater than 50% to call a major variant, and that automatically introduced 'Ns' in low quality or uncertain/uncovered regions of the reference sequence. Eventually, BCFtools [22] v1.11 was utilised to generate the consensus sequences, whereas SARS-CoV-2 clades and haplotypes were called with NextClade [24] Web tool (https://clades.nextstrain.org, accessed on 19 October 2023). The 52 SARS-CoV-2 sequences produced in this study were submitted to the GISAID portal (www.gisaid.org) [25]. Table S2 reports the correspondence of the GISAID IDs of the newly produced sequences with the identifiers reported in this paper.

2.4. Low-frequency variants validation and identification

Twenty-three of the collected samples were sequenced twice to be utilised as controls for minor variants' reproducibility. After performing the viral genome assembly as described above, we analysed all mutations recorded in the Variant Call Format (VCF) files generated using LoFreq [26] v2-1-5 without imposing any restrictions on mutation frequency or strand bias. First, a custom strand filter was applied by requiring a minimum of two forward and two reverse reads supporting each mutation, whereas variants occurring in the first and last one hundred bases were excluded from consideration. To compare the type of the minor variants identified in the replicated samples, the overlap coefficient was calculated for each couple, imposing different frequencies to call minor variants, ranging from 0.5% to 5%, considering the median coverage of each replicate (Venn diagrams provided for 1% frequency only, Figure S2).

2.5. Principal component analysis, PCA

 doi:10.20944/preprints202312.0174.v1

For each group of replicates, the replicate with the highest coverage was chosen to represent the sample. In cases where a sample was sequenced only once, we considered the single available replicate. The final dataset comprised thirty samples, which are summarized in Supplementary Table S2.

The presence of minor mutations reverting to the NC_045512 reference and occurring outside indels was manually evaluated and duly taken into account.

To assess the evolution of minor variants in the immunocompromised and healthy individuals, a Principal Component Analysis (PCA) was conducted using the scikit-learn package (v1.3.0) in Python3.

The dataset used for this analysis includes the list of low-frequency mutations identified in the samples along with their frequency. Before performing the PCA, the mutation frequencies were normalised using the StandardScaler module from the scikit-learn package. The contribution of variance in the resulting principal components (PCs) was also assessed and reported specifically for PC1 and PC2.

3. Results

3.1. Cohort characterisation

A total of 22 patients were enrolled between December 2021 and April 2022, all exhibiting mild COVID-19 symptoms. Eight were classified as immunocompromised individuals (Group 1). This group consisted of three patients with active solid tumours, four patients undergoing chemotherapy for haematological malignancies, and one recent (< 1 year) liver transplant recipient on immunosuppressive therapy. The remaining 14 patients were non-immunocompromised subjects at high risk of COVID-19 clinical progression (Group 2), who presented with various underlying health conditions: three patients had chronic lung disease; six patients had heart disease; one patient had obesity (BMI > 30 kg/m2); one patient had type 2 diabetes mellitus, and three patients had chronic liver disease.

The immunocompromised group presented a mean age of 60 (IQR: 50.5-69), with 75% of males, whereas Group 2 subjects were characterised by a mean age of 72 (IQR: 64.3-83.5) and 50% of males.

All patients were vaccinated 2 doses for SARS-CoV-2, except two in Group1. All Group 2 subjects received a three-days remdesivir therapy, whereas, in Group 1, 2/8 received remdesivir, 5/8 monoclonal antibodies, and one patient was treated with a combination of remdesivir and monoclonal therapy.

Characteristics and clinical information of the studied cohorts are summarised in Table 1.

Table 1. Features of the immunocompromised and the non-immunocompromised cohorts. Information regarding gender, age, type of compromising condition, treatments and vaccination status are reported in the table. Differences in gender and age between the two groups were tested with Fisher exact test. Differences in infection length were tested with Mann-Whitney test.

ID	Gender	Age	Compromising condition	Infection length	Monoclonal Ab	Antivirals	Vaccinated
I_1	M	45	1	21	casirivimab-imdevimab	no	no
I_2	M	64	1	35	casirivimab-imdevimab	no	yes
I_3	F	69	2	21	casirivimab-imdevimab	remdesivir	no
I_4	M	71	2	30	no	remdesivir	yes
I_5	M	49	3	30	bamlanivimab-etesivimab	no	yes
I_6	F	69	1	21	sotrovimab	no	yes
I_7	M	55	1	21	sotrovimab	no	yes
I_8	M	58	2	14	no	remdesivir	yes
Total	8 (M = 75%)						
Mean		**60**					
Median				**25.5**			

Preprints (www.preprints.org) | NOT PEER-REVIEWED | Posted: 4 December 2023 doi:10.20944/preprints202312.0174.v1

H_1	M	37	8	21	no	remdesivir	yes
H_2	M	76	5	14	no	remdesivir	yes
H_3	M	70	6	14	no	remdesivir	yes
H_4	F	82	5	14	no	remdesivir	yes
H_5	M	74	4	14	no	remdesivir	yes
H_6	M	83	5	14	no	remdesivir	yes
H_7	F	59	6	14	no	remdesivir	yes
H_8	F	69	4	14	no	remdesivir	yes
H_9	M	89	5	14	no	remdesivir	yes
H_10	F	66	7	14	no	remdesivir	yes
H_11	F	73	4	14	no	remdesivir	yes
H_12	F	85	5	14	no	remdesivir	yes
H_13	F	48	6	14	no	remdesivir	yes
H_14	M	93	5	14	no	remdesivir	yes
Total	14 (M = 50%)						
Mean		**71.7**					
Median				**14**			
p value	ns	ns		**<0.001**			

1 = Haematological malignancies. 2 = Solid tumour. 3 = Organ transplant. 4 = Chronic lung disease. 5 = Heart disease. 6 = Chronic liver disease. 7 = Diabetes mellitus, type 2. 8 = Obesity (BMI > 30 kg/m^2).

The length of SARS-CoV-2 infection, defined as the time window spanning from the day of the first positive molecular test to the day of the first negative test, was prolonged in immunocompromised patients (25.5 IQR 21-30) compared with the non-immunocompromised subjects (14 IQR:14-14; $p < 0.001$, Mann-Whitney test).

All the swabs that yielded a positive result in the molecular test for detecting SARS-CoV-2 underwent deep sequencing. This involved employing a shotgun methodology on virus-enriched nucleic acids, obtained with SARS-CoV-2 specific probes. In total, 26 and 26 viral full genomes were obtained from the immunocompromised and non-immunocompromised patients, respectively.

Infection lengths of all the subjects and the timepoints for which full-coverage viral sequences were available are summarized in Figure 1. The emergence of mutations over time was monitored at both the consensus level (a mutation must be present in more than 50% of reads covering that position) and the quasispecies level (mutations equal or below the 50% frequency threshold).

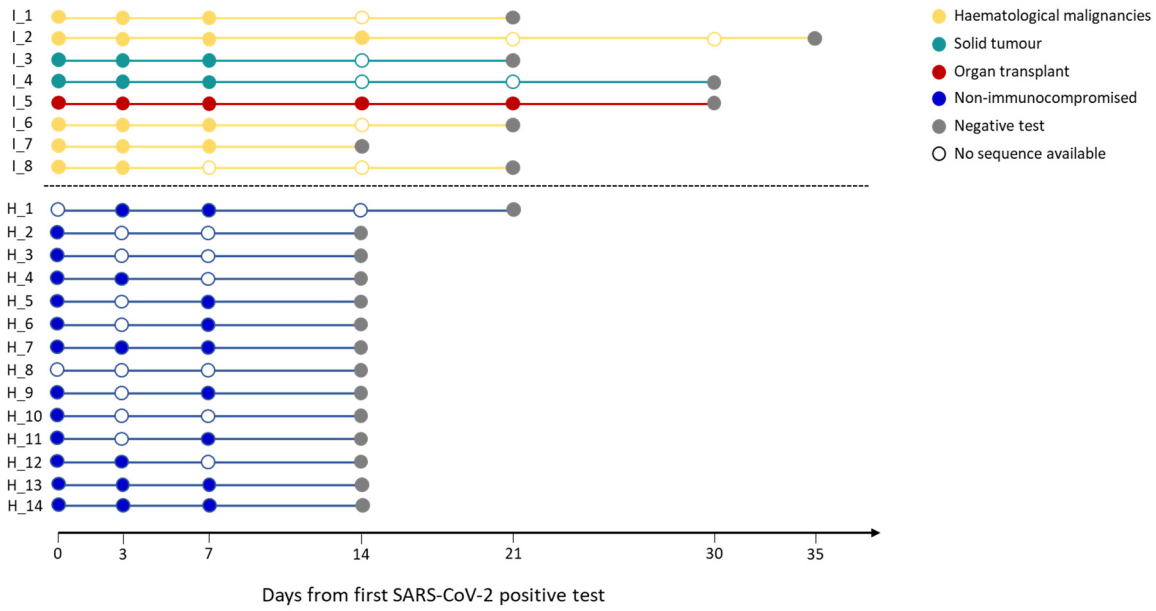

Figure 1. Infection length in immunocompromised and non-immunocompromised subjects. The figure reports the length of the SARS-CoV-2 infection in eight immunocompromised (Group 1) patients and in fourteen non-immunocompromised subjects, but at high-risk of COVID-19 clinical progression (Group 2). The infection length is defined as the time window spanning from the first

 doi:10.20944/preprints202312.0174.v1

day of nasopharyngeal test positivity (day 0) to the first negative nasopharyngeal test. Group 1 subjects are reported in blue, whereas the different immunocompromised subjects are coloured according to the type of compromising condition, provided in the legend. The first negative test is presented as a grey dot. The other dots represent each day at which the subjects were tested, with filled dots indicating the availability of the viral sequence for that timepoint.

3.2. Intra-host variation of SARS-CoV-2 consensus genome in immunocompromised and non-immunocompromised subjects

SARS-CoV-2 intra-host evolution was investigated in seven immunocompromised and in seven non-immunocompromised subjects, according to the availability of viral full genome sequences from multiple timepoints, including at least T0 (the day of the first positive swab) and T7 (the seventh day after the first positive swab). Details about SARS-CoV-2 lineage, number and type of nucleotide and amino acid mutations, together with the timepoint at which the novel mutations were observed, are summarised in Table 2.

As shown in Figure 2, mutations in the viral genome occurred in 3 (42.85%) immunocompromised subjects and in 2 non-immunocompromised (28.57%) subjects. No significant difference in the number of subjects who experienced intra-host viral evolution was observed between the two groups (Fisher exact test, $p = 1$). By considering the same time window, including the timepoints T0 and T7, 2 subjects out of 7 acquired novel viral mutations in both groups, further confirming the lack of difference according to the immune system state.

The immunocompromised subject I_4, a 71-year-old man with pulmonary squamous cell carcinoma, was treated with remdesivir. He was infected with SARS-CoV-2 lineage AY.43 (Delta) [27] and the infection lasted 30 days. After 3 days upon infection, a non-synonymous mutation, 4822A>C (ORF1a:Q1519H), became prevalent and persisted until the end of the infection. Notably the mutation was observed also at T0, but it was slightly below the consensus threshold of 50%, and its frequency increased overtime eventually reaching 100% at T7 (T0: 49.96%, T3: 50.62, T7: 100%). After 7 days from COVID-19 diagnosis, the virus acquired a single nucleotide mutation in the spike gene (22821A>C), resulting in an amino acid change from Aspartic acid to Alanine in position 420 (S: D420A), which was predicted to induce an escaping advantage from the monoclonal antibody LY-CoV016 [28]. At T0, T3 and T7 the frequency of 22821A>C mutation was 0%, 0% and 100%, respectively.

The immunocompromised subject I_5, a 49-years-old man under immunosuppressive therapy due to liver transplant, was treated with bamlanivimab and etesivimab. He was infected with SARS-CoV-2 lineage BA.1 (Omicron) on February 2021 and the infection persisted for 30 days. Full coverage sequences were available after 3, 7, 14 and 21 days, allowing a detailed monitoring of intra-host viral evolution. As a result, for the first two weeks from diagnosis no novel mutations were fixed in the prevailing haplotype, whereas on day 21 a six-nucleotide deletion became prevalent, affecting genomic positions 519-524 and resulting in the deletion of two amino acid residues and one amino acidic change (ORF1a:V84_M85del, ORF1a: E87K). The mutation was not detected at T0, T3 and T7 (0%), it appeared at timepoint 14 at low frequency (6.67%), and was fixed in the consensus sequence at timepoint 21 (53.85% frequency). Interestingly, 519_524del was only one of the several similar deletions that increased in frequency within time in this subject. In fact, as shown in Figure 3 and summarised in Table 3, six different deletions occurring within the viral genomic region 508-524 were competing since timepoint 14, with only one of them eventually prevailing in the subsequent timepoint analysed. In particular, a deletion of 15 nucleotides (508_522del) was detected in 15.44% of reads mapping in that region, and a 9-nucleotide deletion, 510_518del, was present with a frequency of 8.20%. Moreover, a deletion of 6 nucleotides (515_520del) was present with a frequency of 6.49%, and two 3-nucleotide deletions, 516_518del and 518_520del, were present with a frequency of 1.24% and of 1.57%, respectively. These deletions occurred within the Nsp1 coding region and have been reported in literature to correlate with lower viral load and lower serum IFN-β [29].

The third immunocompromised subject to acquire novel viral mutations over time was the subject I_7, a 55-years-old man previously diagnosed with a follicular lymphoma. He was infected with SARS-CoV-2 lineage BA.1.1 (Omicron) and treated with the monoclonal antibody sotrovimab.

Preprints (www.preprints.org) | NOT PEER-REVIEWED | Posted: 4 December 2023 doi:10.20944/preprints202312.0174.v1

After 7 days from the first positive test, subject I_7 acquired two novel mutations, one being silent (4012C>A) and the second one inducing an amino acid change in the ORF1a: 9810C>A, resulting in ORF1a:T3182N. Interestingly, the 4012C>A mutation, was not present at T0, but appeared after 3 days from infection, with a frequency of 42.03%, and reached a frequency of 100% at day 7. Similarly, 9810C>A appeared at T3 with a frequency of 1.43%, and was fixed at T7 with a frequency of 87.50%. SARS-CoV-2 was cleared after 21 days.

The non-immunocompromised subjects displaying intra-host viral evolution were subject H_6 and subject H_9, both subjects were affected by heart disease and cleared the infection within 14 days.

The subject H_6, an 83-years-old man, was infected with BA.2 SARS-CoV-2 lineage (Omicron) and was treated with remdesivir. At day 7, he acquired the synonymous mutation 14602T>C and a deletion of 9 nucleotides in the ORF1a, 510_518del, resulting in three amino acid deletions and one amino acid change: ORF1a: G82_V84del and ORF1a: M85V, respectively. None of the described mutations were present at day 0 at minor frequencies, while at day 7 they were present with a frequency of 75.76% and of 83.33%, respectively.

The subject H_9, an 89-years-old man, was infected with BA.2.9 SARS-CoV-2 lineage (Omicron) and was treated with remdesivir. At day 7 we could observe the reversion of a major synonymous mutation, 25603C>T, that was present at 61.69% at day 0, with the remaining reads supporting the SARS-CoV-2 reference consensus, and that dropped to 17.62% by day 7, with the SARS-CoV-2 reference base prevailing over it (82.77%).

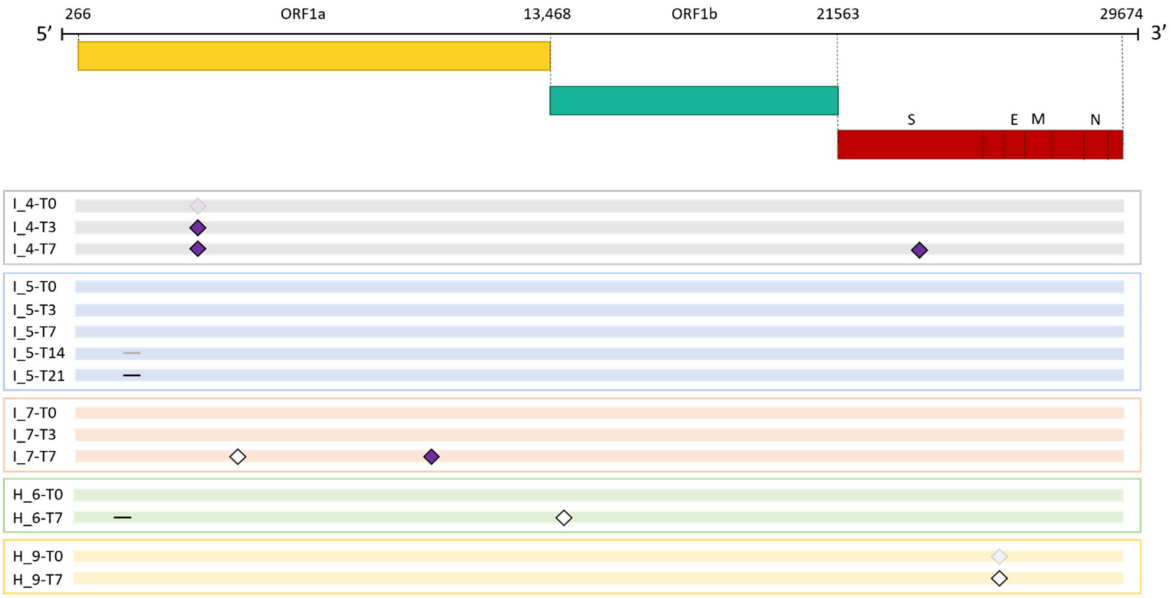

Figure 2. Emergence of SARS-CoV-2 consensus mutations in immunocompromised and non-immunocompromised subjects. The figure shows the longitudinal emergence of viral mutations in three immunocompromised (I) and in two non-immunocompromised (H) subjects. The longitudinal viral sequences of each patient are enclosed in a coloured box and are presented as coloured bars. Only the novel intra-host mutations compared to the T0 are reported. Non-synonymous mutations are depicted as purple-filled diamonds, while silent mutations are presented as white diamonds. Deletions are indicated as black lines. Shaded mutations represent mutations present with a frequency below 50%.

Preprints (www.preprints.org) | NOT PEER-REVIEWED | Posted: 4 December 2023 doi:10.20944/preprints202312.0174.v1

Table 2. SARS-CoV-2 evolution in immunocompromised and non-immunocompromised subjects. The longitudinal emergence of mutations at the consensus level is summarised for the seven immunocompromised and the seven non-immunocompromised subjects with complete genome sequences available for at least timepoints 0 and 7. For each subject, the viral strain identified, the number of acquired mutations, the nucleotide changes and the relative amino acid changes, if present, are reported.

ID	SARS-CoV-2 lineage (PANGO)	Clade (WHO)	Evolved	Novel mutations (N)	Timepoint of novel mutations	Deletions	Nucleotide substitutions	aaMutations
I_1	AY.98.1	Delta	no	-				
I_2	AY.43	Delta	no	-				
I_3	AY.101	Delta	no	-				
I_4	AY.43	Delta	yes	1	T3, T7		4822A>C, 22821A>C	ORF1a:Q1519H, S: D420A
I_5	BA.1	Omicron	yes	1	T21	519_524del		ORF1a: E87K, ORF1a: V84_M85del
I_6	BA.1.1.1	Omicron	no	-				
I_7	BA.1.1	Omicron	yes	2	T7		4012C>A, 9810C>A	silent, ORF1a: T3182N
Total			**3 (42.85%)**					
H_5	BA.2	Omicron	no	-				
H_6	BA.2	Omicron	yes	2	T7	510_518del	14602T>C	ORF1a: M85V, ORF1a: G82_V84del, silent
H_7	BA.1	Omicron	no	-				
H_9	BA.2.9	Omicron	yes	1	T7		25603T>C	silent
H_11	BA.1.1	Omicron	No	-				
H_13	BA.1.1	Omicron	No	-				
H_14	BA.1.1	Omicron	no	-				
Total			**2 (28.57%)**					
p value			**ns**					

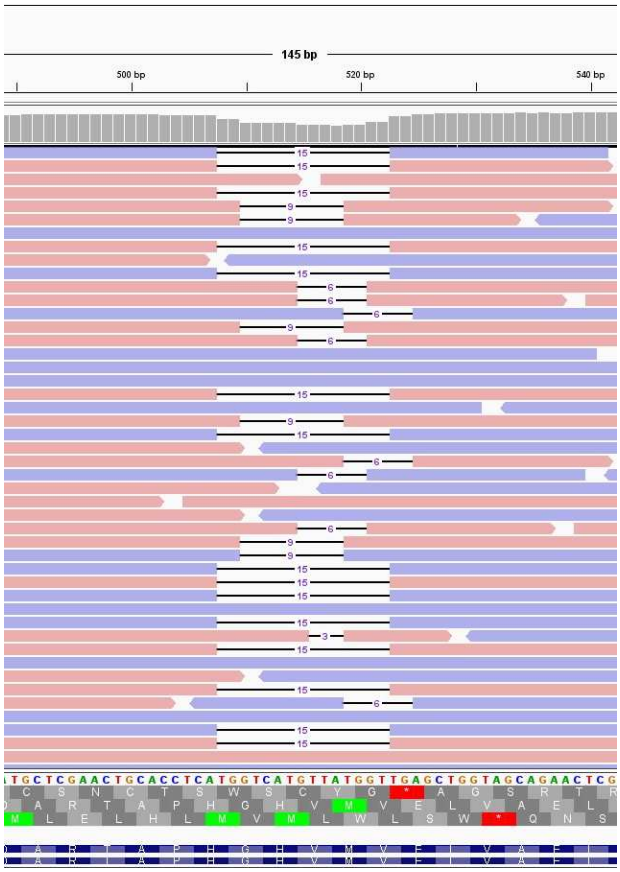

 doi:10.20944/preprints202312.0174.v1

Figure 3. Deletions emerging in subject I_5 at T14. Visualisation of sequence reads spanning the SARS-CoV-2 genomic region 508-524 at T14 of the immunocompromised subject I_5. Reads mapping forward are reported in red, while reverse reads are depicted in blue. The black lines represent deletions, whose length is indicated in figures.

Table 3. Low frequency deletions emerging in subject I_5 at T14. List of low frequency deletions observed in subject I_5 at T14. The deletion becoming prevalent at the subsequent timepoint is depicted in bold. The median coverage of the genomic region 508-524 was of 1698.5 reads per genomic position.

Deletion	Frequency (%)	Haplotype
508_522del	15.44	NSP1_G82del, NSP1_H83del, NSP1V84del, NSP1_M85del, NSP1_V86del
510_518del	8.20	NSP1_G82del, NSP1_H83del, NSP1V84del, NSP1_M85V
515_520del	6.49	
516_518del	1.24	
518_520del	1.57	
519_524del	6.67	NSP1_V84del, NSP1_M85del, NSP1_E87K

3.3. Frequency of emerged non-synonymous mutations in GISAID database

To investigate whether the non-synonymous mutations that emerged in this study cohort had already been reported elsewhere, either before or after, all the human SARS-CoV-2 complete and high-coverage sequences available in GISAID from the beginning of the pandemic to the 15th of October 2023 were downloaded and analysed. Although at very low frequencies, all the investigated mutations were already reported in GISAID database in periods preceding the samples collection for this study (Table S1 and Figure S1). However, the 510_518del was the most frequent and its frequency showed periodic peaks, with the highest peak being reported in September 2023 (Figure S1).

3.4. Analysis of viral quasispecies

After evaluating differences between consensus mutations emerging in the immunocompromised and in the non-immunocompromised subjects, we explored the variation of mutations appearing in the two cohorts at frequencies below or equal to 50%. Prior to performing any comparison between the groups, we defined the parameters for minor variants to be reliable and reproducible, thanks to the availability of deeply sequenced technical replicates of several samples.

3.4.1. Validation of the detection pipeline for low-frequency mutations

Twenty-three of the collected samples were sequenced twice to be utilised as controls for minor variants' reproducibility. All mutations recorded in the Variant Call Format (VCF) files, generated using LoFreq v2-1-5 without imposing any restrictions on mutation frequency or strand bias, were analysed. To compare the minor variants identified in the technical replicates, the overlap coefficient was calculated, imposing different minimum frequencies for minor variants calling, ranging from 0.5% to 5% (Supplementary Figure 2a, provided applying 1% frequency to call minor variants). In addition, we assessed the impact of the sequencing depth on the overlap coefficient (Supplementary Figure 2b). Finally, we investigated the potential correlation between the number of minor variants observed in each sample and the median sequencing depth (Figure S3). Although a strong correlation was observed at low depths ($r_{Spearman} = 0.8$, $p = 0.0009$), for samples with median sequencing depth equal or higher than 600 reads per genomic position the two variables were independent ($r_{Spearman} = -0.30$, $p = 0.16$). As a result, we defined the best combination of the minimum frequency and median sequencing depth parameters for reproducible minor variants calling, being of 1% and 600 reads per genomic position, respectively. Accordingly, only samples satisfying this requirement were considered for minor variants analysis, and only mutations with a frequency between 1% and 50% included were contemplated.

Preprints (www.preprints.org) | NOT PEER-REVIEWED | Posted: 4 December 2023 doi:10.20944/preprints202312.0174.v1

3.4.2. Quantitative analysis of minor variants

Given that some subjects were infected with Omicron, whereas others were infected with Delta, we checked the potential impact of different viral variants in the number of detected low-frequency mutations. The analysis confirmed that no difference can be attributed to viral variants, as shown in the comparison between Omicron and Delta viral samples of immunocompromised subjects at T0 (Figure S4a). Accordingly, we proceeded by accounting the immunological status as the only variable to be assessed, regardless of the SARS-CoV-2 variant of infection. To investigate whether the immunocompromised subjects were more prone to develop novel mutations, we compared the number of minor variants observed overall, at T0, and at T7 in the immunocompromised and in the non-immunocompromised subjects (Figure 4a–c). No significant differences emerged between the median number of minor variants at T0 (N_I=7, N_H=9, p = 0.09, Mann-Whitney test), at T7 (N_I=3, N_H=3, p = 1, Mann-Whitney test) or overall (N_I = 16, N_H = 14, p = 0.08, Mann-Whitney test). For three immunocompromised and two non-immunocompromised subjects it was possible to assess the longitudinal changes in the number of minor variants identified between T0 and T7(Figure 4d). Accordingly, although the number of the considered subjects is limited, trends in the variation of the number of minor variants seem to be subject-dependent, regardless of the status of the immune system.

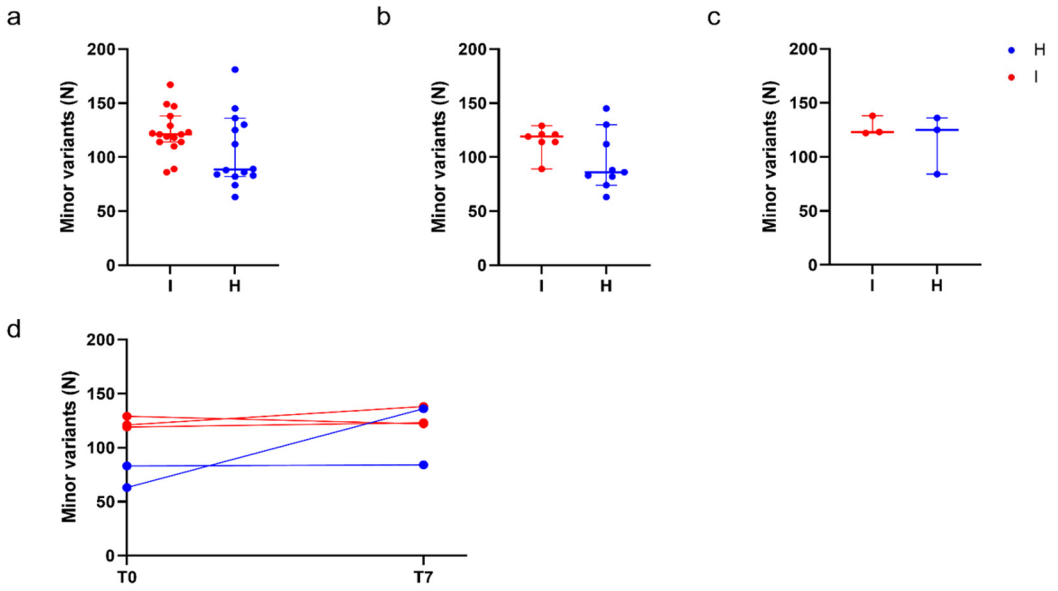

Figure 4. Quantitative analysis of minor variants. Comparison of the number of minor variants identified in immunocompromised (I) and in non-immunocompromised (H) subjects. (**a**) Comparison of the number of minor variants identified in immunocompromised and non-immunocompromised subjects, regardless of the timepoint at which the samples were collected (N_I=16, Median $_I$=121.0, N_H =14, Median $_H$=88.50, p = 0.08, Mann-Whitney test). (**b**) Comparison of the number of minor variants identified in immunocompromised and non-immunocompromised subjects at T0 (N_I=7, Median $_I$= 119.0, N_H=9, Median $_H$=86.0, p = 0.09, Mann-Whitney test). (**c**) Comparison of the number of minor variants identified in immunocompromised subjects and non-immunocompromised subjects at T7 (N_I=3, Median $_I$= 123.0, N_H=3, Median $_H$=125.0, p = 1, Mann-Whitney test). (**d**) Longitudinal intra-host variation of the number of minor variants identified in subjects for which T0 and T7 samples were available (N_I = 3, N_H = 2). The number of minor variants detected in each sample of an immunocompromised subjects are reported as red dots. Conversely, the number of minor variants detected in each sample of a non-immunocompromised subject are reported as blue dots, according to the legend.

Preprints (www.preprints.org) | NOT PEER-REVIEWED | Posted: 4 December 2023 doi:10.20944/preprints202312.0174.v1

3.4.3. Qualitative analyses of minor variants

After demonstrating that the number of minor variants does not differ between immunocompromised and non-immunocompromised subjects, we assessed whether the type of mutations and their frequency was different in the two groups by performing a principal component analysis. Firstly, we ensured that, among the immunocompromised subjects, there was no difference in the minor variants profile according to the SARS-CoV-2 variant of infection (Figure S4b). Then, we generated a principal component analysis for all samples at T0, at T7 and regardless of the timepoints, considering the type and frequency of minor variants identified in each sample (Figure 5a–c). As a result, data did not cluster differently according to the immunological status. Although in some panels, such as panel a, most of the data seem to cluster in two different groups, the variance explained by the first two principal components is very low (less than 30%), further confirming the absence of a significant difference in minor variants profile of immunocompromised subjects compared to non-immunocompromised ones. Finally, we monitored the conservation of low-frequency mutations over time in two immunocompromised patients, to understand the dynamics of viral quasispecies composition. As shown in Figure 5d,e, the number of mutations fluctuates but is relatively stable between consecutive timepoints (grey dashed lines); nonetheless, there are always new mutations appearing (red lines in the plots) and replacing a portion of those that were present in previous samples (blue lines), suggesting that the quasispecies population undergoes intense renewal, especially in persistent infections.

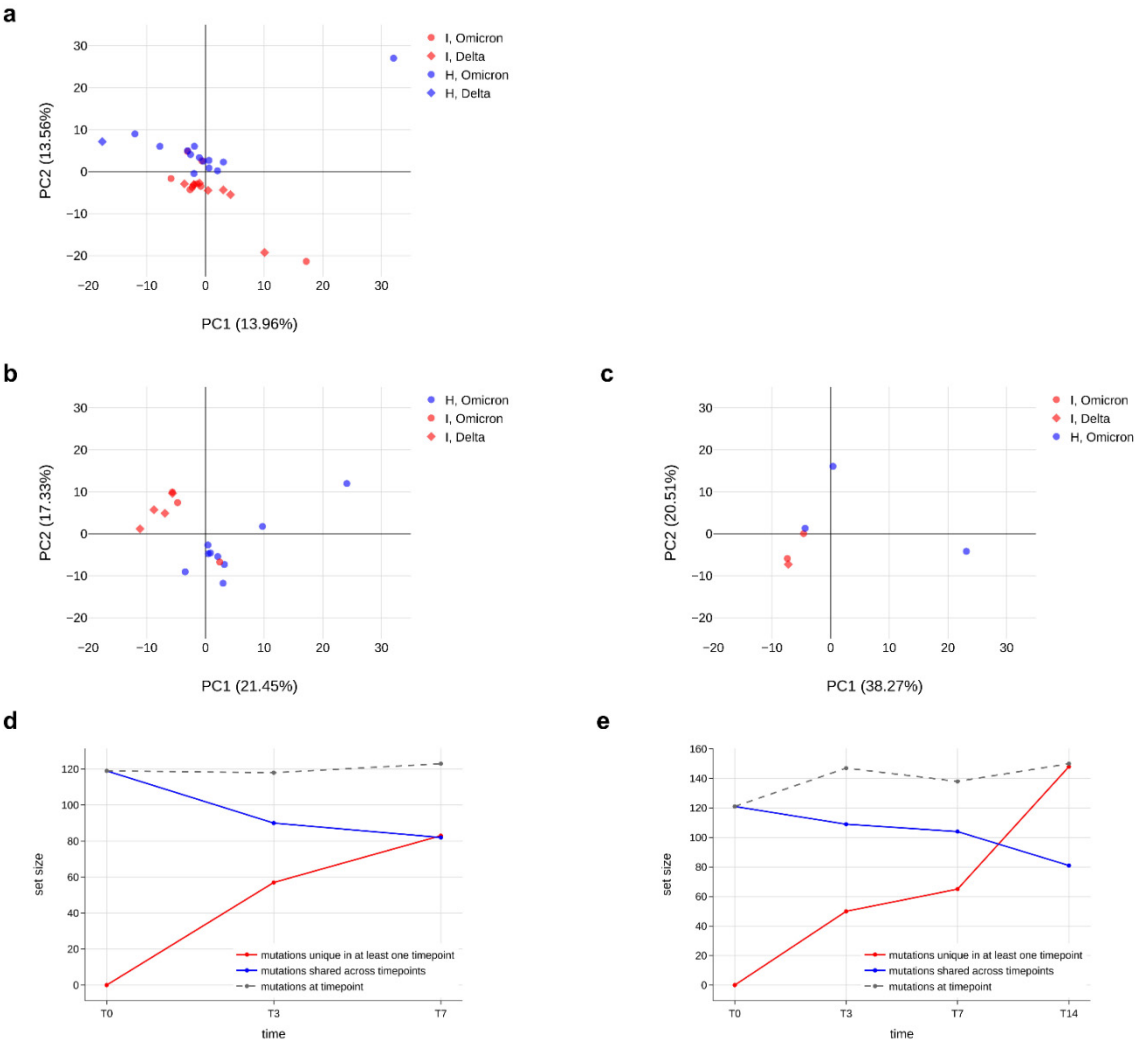

 doi:10.20944/preprints202312.0174.v1

Figure 5. Minor variants profile of immunocompromised and non-immunocompromised subjects. (**a**–**c**) Principal component analysis (PCA) of all the minor variants observed in samples collected from either the immunocompromised or the non-immunocompromised subjects at any timepoint (**a**); at T0 (**b**) and at T7 (**c**). According to the legend, minor variants profiles of immunocompromised subjects are provided as red dots, whereas the ones of non-immunocompromised subjects are presented as blue dots. Profiles of subjects infected with Delta variant are represented as diamonds, whereas dots indicate Omicron as the variant of infection. The variation explained by each PC is provided along the relative axis. (**d**,**e**) Longitudinal analysis of the minor variants that persisted in all the considered timepoints (blue line), of the minor variants identified at least at one timepoint (red line) and of the minor variants specific of each specific timepoint in the subject I_3 (**d**) and in the subject I_5 (**e**).

4. Discussion

In this study, SARS-CoV-2 nasopharyngeal samples were collected at multiple timepoints from a group of eight immunocompromised subjects and from a group of fourteen non-immunocompromised subjects to investigate the impact of a compromised immune system on SARS-CoV-2 intra-host evolution. The immunocompromised group included subjects with haematological malignancies, subjects with solid tumours, or organ transplant recipients receiving an immunosuppressive therapy. All the non-immunocompromised subjects received a remdesivir therapy, whereas the immunocompromised subjects received remdesivir, monoclonal antibodies, or a combination thereof.

Each sample was deep sequenced through the Twist SARS-CoV-2 Research Panel enrichment protocol to ensure a complete profiling of the target sequences and to obtain an unbiased representation of intra-sample variants. As a matter of fact, amplicon-based sequencing often leads to biased amplification across the genome due to differences in primer efficiency and affinity, especially in case of mismatches in the annealing regions [17,18]. More importantly, amplicon sequencing has been recently proven to provide a highly biased representation of minor allele frequencies [18]. Conversely, given that enrichment methods are based on a larger number of probes than amplicon-based methods and can tolerate up to 20% of mismatches [30], capture-based methods are more robust and provide a reliable representation of intra-sample low-frequency variants [17,18]. Moreover, among the most popular SARS-CoV-2 enrichment panels available, we have opted for the SARS-CoV-2-specific panel of Twist Bioscience, which was proven to be the most sensitive and efficient [19]. To further improve the accuracy of the enrichment method applied in the current study, the number of PCR amplification cycles, which is known to be a source of artefacts, was minimised to 10 cycles during library preparation and to 9 cycles after the probe-based enrichment, being comparable with the number of amplification cycles normally performed for metatranscriptomic sequencing [18].

As a result, we obtained a total of 52 consensus sequences from 21 subjects (no sequencing results were obtained for one patient out of the 22 initially enrolled), with 4 out of 8 immunocompromised subjects and 1 out of 13 non-immunocompromised subjects being infected with Delta variant. The remaining subjects were infected with Omicron variant.

All the subjects for whom the complete SARS-CoV-2 consensus sequence was available for at least T0 and T7 were assessed for intra-host viral evolution, resulting in 7 immunocompromised and 7 non-immunocompromised subjects. Although, as expected, immunocompromised subjects showed a prolonged infection compared with non-immunocompromised subjects (25.5 and 14 days of median infection length in immunocompromised and non-immunocompromised subjects, respectively, $p < 0.001$, Mann-Whitney test), no differences in the amount or type of major mutations emerged during the infection was observed between the two groups. As a matter of fact, three immunocompromised subjects out of seven (42.85%) and two non-immunocompromised subjects out of seven (28.57%) acquired novel mutations during the viral infection. Specifically, 2 out of 7 immunocompromised and 2 out of 7 non-immunocompromised subjects acquired a novel mutation within 7 days, suggesting the length of infection as the major driver for the intra-host accumulation of mutations. In particular, the subject H_9 acquired a synonymous mutation in ORF3b, while the

 doi:10.20944/preprints202312.0174.v1

subject H_6 acquired a synonymous mutation in the ORF1ab, specifically within the gene of the RNA-dependent RNA polymerase, and a 9-nucleotide deletion, 510_518del, resulting in three amino acids deletion, NSP1_G82_V84del, and an amino acid substitution, NSP1_M85V. Interestingly, this deletion was detected in SARS-CoV-2 sequences deposited in GISAD with a fluctuating frequency that peaked at 1.76% on September 2023. Moreover, the same mutation was detected at low frequency in the immunocompromised subject I_5, who only received bamlanivimab-etesivimab treatment, and where 5 different deletions occurring within the genomic region 508-524 were competing at T14, with 519_524del becoming prevalent at T21. A previous work [29] defined the 500-532 Nsp1 locus as a deletion hotspot, with deletions variants being detected in 37 countries worldwide, and correlated such deletions to lower viral load and lower serum INF-β. The acquisition within time of similar deletions in the same hotspot, regardless of the immune system status and/or treatment received, further supports the hypothesis that the compromised immune system alone does not affect SARS-CoV-2 type or amount of novel mutations acquired. Other two subjects acquired novel SARS-CoV-2 mutations during the monitoring carried out in this study: the subject I_4, who acquired two non-synonymous mutations, ORF1a:Q1519H and S: D420A, and the subject I_7, who acquired a silent mutation and a non-synonymous mutation, ORF1a: T3182N. The ORF1a:Q1519H substitution has not been reported in literature, however it occurs within the gene of Nsp3 protein. Nsp3 is the largest protein encoded by SARS-CoV-2, comprising up to 16 different domains and regions and it is essential for viral replication and transcription [31]. It participates in polyproteins processing, it interacts with the nucleocapsid protein and it binds viral RNA [31,32]. It has a critical role in counteracting host innate immunity as well, due to its de-ADP-ribosylating, de-ubiquitinating, and de-ISGylating activities [31]. Accordingly, it is a target of antiviral drugs, such as remdesivir [31–34]. Given that the subject I_4 was treated with remdesivir, an antiviral that has previously been suggested to foster viral evolution [8,9,15,34], the treatment might have promoted the emergence of such mutation. The subject I_4 also acquired a mutation within the Spike protein, D420A, which was suggested in literature to enable bamlanivimab and etesevimab monoclonal antibodies escape in silico [28]. Subject I_7, instead, acquired a silent mutation within Nsp2 protein and a non-synonymous mutation within the ORF1a, T3182N, which lies in the Nsp3 protein, previously mentioned. Overall, no significant differences emerged in the number of subjects experiencing intra-host viral evolution nor in the amount of synonymous and non-synonymous mutations acquired within the infection (Fischer exact test, $p > 0.05$).

We further explored the intra-host viral evolution by assessing the mutations occurring at low frequency. After validating and ensuring the reliability and consistency of the minor variants identified in replicated samples, we analysed all variants with a frequency ranging from 1% to 50% of samples showing a median coverage greater than 600 reads per genomic region. As a result, 30 out of the 52 samples were investigated for minor variants. Accordingly, no significant differences were observed in the amount and in the profile of minor variants identified in immunocompromised and non-immunocompromised subjects, nor between subjects infected with Delta or Omicron variants. Thus, minor variants analysis further supports the results of the consensus analysis, suggesting that the immune system state alone does not affect SARS-CoV-2 intra-host variability. Similarly, no clear impact of specific antiviral treatments was observed.

The main limitations of this study are the low number of subjects recruited and successfully sequenced and the relatively short infection lengths observed in both groups, probably due to the SARS-CoV-2 variant of infection the effect of vaccines and antiviral treatments [35].

On the other hand, the study setting and methodologies chosen in this work diverge from most of the previous studies investigating the effects of immune system deficiencies on SARS-CoV-2 evolution [1,3–5]. In fact, all studies concerning low frequency mutations differ for the choice of sequencing protocols and data analysis pipelines, with most of the works relying on amplicon sequencing, which has been reported to be strongly biased for low frequency representation. Moreover, most of these studies lack a validation step, essential to calibrate low frequency variant calling parameters, opting instead for arbitrary frequency and coverage thresholds. In addition, most studies focus on a single immunocompromised patient, whereas very few consider also

immunocompetent subjects or subjects with other comorbidities [12,13,15,16]. Given that non-immunocompromised subjects generally don't experience severe symptoms or hospitalisation, persistent infection in such subjects are very rarely investigated, hindering a fair comparison with immunocompromised subjects and leading to a literature biased toward the latter. However, some research groups previously investigated SARS-CoV-2 intra-host evolution in immunocompetent subjects experiencing prolonged infection, reporting the longitudinal emergence of novel mutations including immune escaping mutations [12,15]. Similarly, other groups reported SARS-CoV-2 accumulation of mutations at the consensus level or at low frequencies in immunocompetent subjects in shorter time windows [13,16].

Overall, our data directly compare longitudinal intra-host SARS-CoV-2 diversity in immunocompromised and non-immunocompromised subjects, demonstrating that there are no disparities in the speed of new mutation emergence or in the type of mutations acquired between the two groups.

Supplementary Materials: The following supporting information can be downloaded at: https://github.com/MedCompUnipd/SARS-CoV-2_immunocompromised, Figure S1: Frequency of the emerged non-synonymous mutations in GISAID; Figure S2: Minor variants reproducibility; Figure S3: Correlation between minor variants and median coverage; Figure S4: Delta and Omicron minor variants are comparable in number and type; Table S1: Monthly frequency of SARS-CoV-2 sequences available in GISAID and carrying either NSP3_Q701H, NSP4_T419N, S: D420A, 519_524del or 510_518del; Table S2: Full list of samples ID, collection data, consensus sequence availability and fulfilment of criteria for minor variants analysis.

Author Contributions: Conceptualization, S.T. and E.L.; methodology, L.M., M.B., E.V., M.A., G.C., M.C., G.M. and M.P.; software, L.M., M.B., E.V. and G.M.; validation, L.M., M.B., E.V., G.M., M.A., G.C., M.C. and M.P.; formal analysis, L.M., M.B., G.M. and E.V.; data curation, L.M., M.B., E.V., G.M., M.A., M.C., G.C. and M.P.; resources, L.S., A.M.C., S.T. and E.L.; visualization, L.M. and M.B.; original draft preparation, L.M. and E.L.; writing—review and editing, S.T., A.M.C., L.S., M.P., L.M., M.B., E.V. and E.L.; supervision, A.M.C., S.T. and E.L.; funding acquisition, S.T. and E.L. All authors have read and agreed to the published version of the manuscript.

Funding: This research was funded by the University of Padova (Italy), grant number PRID/SID 2020 to E.L. and by the Italian Ministry of University and Research (PRIN 2020), grant number 2020XFNCP7, to S.T.

Institutional Review Board Statement: The study was conducted in accordance with the Declaration of Helsinki and was approved by the Ethics Committee for Clinical Research of the province of Padua under protocol number CESC code 4923/AO/20, approval Date 24/09/2020.

Informed Consent Statement: Study participation was by written consent. No participants are under 18 years of age.

Data Availability Statement: The data presented in this study are openly available in GISAID repository at doi:10.55876/gis8.231130qo. The GISAID data availability table is available at https://github.com/MedCompUnipd/SARS-CoV-2_immunocompromised

Acknowledgments: We gratefully acknowledge the authors from the originating laboratories and the submitting laboratories who generated and shared, via GISAID, the data on which part of this research is based.

Conflicts of Interest: The authors declare no conflict of interest.

References

1. Choi, B.; Choudhary, M.C.; Regan, J.; Sparks, J.A.; Padera, R.F.; Qiu, X.; Solomon, I.H.; Kuo, H.-H.; Boucau, J.; Bowman, K.; et al. Persistence and Evolution of SARS-CoV-2 in an Immunocompromised Host. *N Engl J Med* **2020**, *383*, 2291–2293, doi:10.1056/NEJMc2031364.
2. Beran, A.; Zink, E.; Mhanna, M.; Abugharbyeh, A.; Hanrahan, J.; Duggan, J.; Assaly, R. Transmissibility and Viral Replication of SARS-COV-2 in Immunocompromised Patients. *J Med Virol* **2021**, *93*, 4156–4160, doi:10.1002/jmv.26970.
3. Avanzato, V.A.; Matson, M.J.; Seifert, S.N.; Pryce, R.; Williamson, B.N.; Anzick, S.L.; Barbian, K.; Judson, S.D.; Fischer, E.R.; Martens, C.; et al. Case Study: Prolonged Infectious SARS-CoV-2 Shedding from an Asymptomatic Immunocompromised Individual with Cancer. *Cell* **2020**, *183*, 1901-1912.e9, doi:10.1016/j.cell.2020.10.049.

4. Quaranta, E.G.; Fusaro, A.; Giussani, E.; D'Amico, V.; Varotto, M.; Pagliari, M.; Giordani, M.T.; Zoppelletto, M.; Merola, F.; Antico, A.; et al. SARS-CoV-2 Intra-Host Evolution during Prolonged Infection in an Immunocompromised Patient. *International Journal of Infectious Diseases* **2022**, *122*, 444–448, doi:10.1016/j.ijid.2022.06.023.
5. Kemp, S.A.; Collier, D.A.; Datir, R.P.; Ferreira, I.A.T.M.; Gayed, S.; Jahun, A.; Hosmillo, M.; Rees-Spear, C.; Mlcochova, P.; Lumb, I.U.; et al. SARS-CoV-2 Evolution during Treatment of Chronic Infection. *Nature* **2021**, *592*, 277–282, doi:10.1038/s41586-021-03291-y.
6. Ma, W.; Yang, J.; Fu, H.; Su, C.; Yu, C.; Wang, Q.; de Vasconcelos, A.T.R.; Bazykin, G.A.; Bao, Y.; Li, M. Genomic Perspectives on the Emerging SARS-CoV-2 Omicron Variant. *Genomics, Proteomics & Bioinformatics* **2022**, *20*, 60–69, doi:10.1016/j.gpb.2022.01.001.
7. Hill, V.; Du Plessis, L.; Peacock, T.P.; Aggarwal, D.; Colquhoun, R.; Carabelli, A.M.; Ellaby, N.; Gallagher, E.; Groves, N.; Jackson, B.; et al. The Origins and Molecular Evolution of SARS-CoV-2 Lineage B.1.1.7 in the UK. *Virus Evolution* **2022**, *8*, veac080, doi:10.1093/ve/veac080.
8. Szemiel, A.M.; Merits, A.; Orton, R.J.; MacLean, O.A.; Pinto, R.M.; Wickenhagen, A.; Lieber, G.; Turnbull, M.L.; Wang, S.; Furnon, W.; et al. In Vitro Selection of Remdesivir Resistance Suggests Evolutionary Predictability of SARS-CoV-2. *PLOS Pathogens* **2021**, *17*, e1009929, doi:10.1371/journal.ppat.1009929.
9. Gandhi, S.; Klein, J.; Robertson, A.J.; Peña-Hernández, M.A.; Lin, M.J.; Roychoudhury, P.; Lu, P.; Fournier, J.; Ferguson, D.; Mohamed Bakhash, S.A.K.; et al. De Novo Emergence of a Remdesivir Resistance Mutation during Treatment of Persistent SARS-CoV-2 Infection in an Immunocompromised Patient: A Case Report. *Nat Commun* **2022**, *13*, 1547, doi:10.1038/s41467-022-29104-y.
10. Rockett, R.; Basile, K.; Maddocks, S.; Fong, W.; Agius, J.E.; Johnson-Mackinnon, J.; Arnott, A.; Chandra, S.; Gall, M.; Draper, J.; et al. Resistance Mutations in SARS-CoV-2 Delta Variant after Sotrovimab Use. *New England Journal of Medicine* **2022**, *386*, 1477–1479, doi:10.1056/NEJMc2120219.
11. Vellas, C.; Del Bello, A.; Debard, A.; Steinmeyer, Z.; Tribaudeau, L.; Ranger, N.; Jeanne, N.; Martin-Blondel, G.; Delobel, P.; Kamar, N.; et al. Influence of Treatment with Neutralizing Monoclonal Antibodies on the SARS-CoV-2 Nasopharyngeal Load and Quasispecies. *Clinical Microbiology and Infection* **2022**, *28*, 139.e5-139.e8, doi:10.1016/j.cmi.2021.09.008.
12. Voloch, C.M.; da Silva Francisco Jr, R.; de Almeida, L.G.P.; Brustolini, O.J.; Cardoso, C.C.; Gerber, A.L.; Guimarães, A.P. de C.; Leitão, I. de C.; Mariani, D.; Ota, V.A.; et al. Intra-Host Evolution during SARS-CoV-2 Prolonged Infection. *Virus Evolution* **2021**, *7*, veab078, doi:10.1093/ve/veab078.
13. Manuto, L.; Grazioli, M.; Spitaleri, A.; Fontana, P.; Bianco, L.; Bertolotti, L.; Bado, M.; Mazzotti, G.; Bianca, F.; Onelia, F.; et al. Rapid SARS-CoV-2 Intra-Host and Within-Household Emergence of Novel Haplotypes. *Viruses* **2022**, *14*, 399, doi:10.3390/v14020399.
14. De Marco, C.; Marascio, N.; Veneziano, C.; Biamonte, F.; Trecarichi, E.M.; Santamaria, G.; Leviyang, S.; Liberto, M.C.; Mazzitelli, M.; Quirino, A.; et al. Whole-Genome Analysis of SARS-CoV-2 in a 2020 Infection Cluster in a Nursing Home of Southern Italy. *Infection, Genetics and Evolution* **2022**, *99*, 105253, doi:10.1016/j.meegid.2022.105253.
15. Heyer, A.; Günther, T.; Robitaille, A.; Lütgehetmann, M.; Addo, M.M.; Jarczak, D.; Kluge, S.; Aepfelbacher, M.; Schulze Zur Wiesch, J.; Fischer, N.; et al. Remdesivir-Induced Emergence of SARS-CoV2 Variants in Patients with Prolonged Infection. *Cell Reports Medicine* **2022**, *3*, 100735, doi:10.1016/j.xcrm.2022.100735.
16. Lythgoe, K.A.; Hall, M.; Ferretti, L.; de Cesare, M.; MacIntyre-Cockett, G.; Trebes, A.; Andersson, M.; Otecko, N.; Wise, E.L.; Moore, N.; et al. SARS-CoV-2 within-Host Diversity and Transmission. *Science* **2021**, *372*, eabg0821, doi:10.1126/science.abg0821.
17. Chiara, M.; D'Erchia, A.M.; Gissi, C.; Manzari, C.; Parisi, A.; Resta, N.; Zambelli, F.; Picardi, E.; Pavesi, G.; Horner, D.S.; et al. Next Generation Sequencing of SARS-CoV-2 Genomes: Challenges, Applications and Opportunities. *Briefings in Bioinformatics* **2021**, *22*, 616–630, doi:10.1093/bib/bbaa297.
18. Xiao, M.; Liu, X.; Ji, J.; Li, M.; Li, J.; Yang, L.; Sun, W.; Ren, P.; Yang, G.; Zhao, J.; et al. Multiple Approaches for Massively Parallel Sequencing of SARS-CoV-2 Genomes Directly from Clinical Samples. *Genome Medicine* **2020**, *12*, 57, doi:10.1186/s13073-020-00751-4.
19. Rehn, A.; Braun, P.; Knüpfer, M.; Wölfel, R.; Antwerpen, M.H.; Walter, M.C. Catching SARS-CoV-2 by Sequence Hybridization: A Comparative Analysis. *mSystems* **2021**, *6*, 10.1128/msystems.00392-21, doi:10.1128/msystems.00392-21.
20. Antinori, A.; Bausch-Jurken, M. The Burden of COVID-19 in the Immunocompromised Patient: Implications for Vaccination and Needs for the Future. *J Infect Dis* **2023**, *228*, S4–S12, doi:10.1093/infdis/jiad181.
21. Bolger, A.M.; Lohse, M.; Usadel, B. Trimmomatic: A Flexible Trimmer for Illumina Sequence Data. *Bioinformatics* **2014**, *30*, 2114–2120, doi:10.1093/bioinformatics/btu170.
22. Danecek, P.; Bonfield, J.K.; Liddle, J.; Marshall, J.; Ohan, V.; Pollard, M.O.; Whitwham, A.; Keane, T.; McCarthy, S.A.; Davies, R.M.; et al. Twelve Years of SAMtools and BCFtools. *GigaScience* **2021**, *10*, giab008, doi:10.1093/gigascience/giab008.

23. VarScan 2: Somatic Mutation and Copy Number Alteration Discovery in Cancer by Exome Sequencing Available online: https://genome.cshlp.org/content/22/3/568 (accessed on 1 December 2023).
24. Aksamentov, I.; Roemer, C.; Hodcroft, E.B.; Neher, R.A. Nextclade: Clade Assignment, Mutation Calling and Quality Control for Viral Genomes. *Journal of Open Source Software* **2021**, *6*, 3773, doi:10.21105/joss.03773.
25. Khare, S.; Gurry, C.; Freitas, L.; Schultz, M.B.; Bach, G.; Diallo, A.; Akite, N.; Ho, J.; Lee, R.T.; Yeo, W.; et al. GISAID's Role in Pandemic Response. *CCDCW* **2021**, *3*, 1049–1051, doi:10.46234/ccdcw2021.255.
26. Wilm, A.; Aw, P.P.K.; Bertrand, D.; Yeo, G.H.T.; Ong, S.H.; Wong, C.H.; Khor, C.C.; Petric, R.; Hibberd, M.L.; Nagarajan, N. LoFreq: A Sequence-Quality Aware, Ultra-Sensitive Variant Caller for Uncovering Cell-Population Heterogeneity from High-Throughput Sequencing Datasets. *Nucleic Acids Res* **2012**, *40*, 11189–11201, doi:10.1093/nar/gks918.
27. Rambaut, A.; Holmes, E.C.; O'Toole, Á.; Hill, V.; McCrone, J.T.; Ruis, C.; du Plessis, L.; Pybus, O.G. A Dynamic Nomenclature Proposal for SARS-CoV-2 Lineages to Assist Genomic Epidemiology. *Nat Microbiol* **2020**, *5*, 1403–1407, doi:10.1038/s41564-020-0770-5.
28. Laurini, E.; Marson, D.; Aulic, S.; Fermeglia, A.; Pricl, S. Molecular Rationale for SARS-CoV-2 Spike Circulating Mutations Able to Escape Bamlanivimab and Etesevimab Monoclonal Antibodies. *Sci Rep* **2021**, *11*, 20274, doi:10.1038/s41598-021-99827-3.
29. Lin, J.; Tang, C.; Wei, H.; Du, B.; Chen, C.; Wang, M.; Zhou, Y.; Yu, M.; Cheng, L.; Kuivanen, S.; et al. Genomic Monitoring of SARS-CoV-2 Uncovers an Nsp1 Deletion Variant That Modulates Type I Interferon Response. *Cell Host & Microbe* **2021**, *29*, 489-502.e8, doi:10.1016/j.chom.2021.01.015.
30. Genomic Sequencing of SARS-CoV-2: A Guide to Implementation for Maximum Impact on Public Health Available online: https://www.who.int/publications-detail-redirect/9789240018440 (accessed on 9 November 2023).
31. Lei, J.; Kusov, Y.; Hilgenfeld, R. Nsp3 of Coronaviruses: Structures and Functions of a Large Multi-Domain Protein. *Antiviral Research* **2018**, *149*, 58–74, doi:10.1016/j.antiviral.2017.11.001.
32. Armstrong, L.A.; Lange, S.M.; Cesare, V.D.; Matthews, S.P.; Nirujogi, R.S.; Cole, I.; Hope, A.; Cunningham, F.; Toth, R.; Mukherjee, R.; et al. Biochemical Characterization of Protease Activity of Nsp3 from SARS-CoV-2 and Its Inhibition by Nanobodies. *PLOS ONE* **2021**, *16*, e0253364, doi:10.1371/journal.pone.0253364.
33. Aleebrahim-Dehkordi, E.; Ghoshouni, H.; Koochaki, P.; Esmaili-Dehkordi, M.; Aleebrahim, E.; Chichagi, F.; Jafari, A.; Hanaei, S.; Heidari-Soureshjani, E.; Rezaei, N. Targeting the Vital Non-Structural Proteins (NSP12, NSP7, NSP8 and NSP3) from SARS-CoV-2 and Inhibition of RNA Polymerase by Natural Bioactive Compound Naringenin as a Promising Drug Candidate against COVID-19. *Journal of Molecular Structure* **2023**, *1287*, 135642, doi:10.1016/j.molstruc.2023.135642.
34. Jung, L.S.; Gund, T.M.; Narayan, M. Comparison of Binding Site of Remdesivir and Its Metabolites with NSP12-NSP7-NSP8, and NSP3 of SARS CoV-2 Virus and Alternative Potential Drugs for COVID-19 Treatment. *Protein J* **2020**, *39*, 619–630, doi:10.1007/s10930-020-09942-9.
35. Puhach, O.; Meyer, B.; Eckerle, I. SARS-CoV-2 Viral Load and Shedding Kinetics. *Nat Rev Microbiol* **2023**, *21*, 147–161, doi:10.1038/s41579-022-00822-w.